Setturu et al., Geoinfor Geostat: An Overview 2013, 1:4
http://dx.doi.org/10.4172/2327-4581.1000112

Geoinformatics & Geostatistics: An Overview

Research Article

A SCITECHNOL JOURNAL

Land Surface Temperature Responses to Land Use Land Cover Dynamics

Bharath Setturu[1,2], Rajan KS[2] and Ramachandra TV[1,3]*

Abstract

Land use and land cover (LULC) changes induced by human or natural processes drive biogeochemistry of the Earth influencing the climate at global as well as regional scales. Drastic changes in the land cover with the decline in vegetation and water bodies due to anthropogenic activities enhances the heat emission from land surface and atmospheric temperatures Increased land surface temperature (LST) is mainly due to increase in concentrated human activities, paved land cover or barren lands. Due to complexity of landscapes the sampling was difficult to derive LST and environmental response relationships. Temporal data acquired through space borne remote sensors has bridged the gap of temporal data for the entire earth surface. The current study explores the relation between surface biophysical parameters to sub-pixel thermal variations. The thermal infrared bands of remote sensing data help to retrieve LST, which are supplemented by ground based measurements. Analysis of LST with LULC indicates a negative correlation between vegetation indices and LST. The general trend in the ambient temperature of Uttara Kannada over the 31 year period was established. It clarifies that there was a fundamental drift of temperature rise in recent years, especially during the last decade.

Keywords: Land surface temperature; Land use; Land cover; Emissivity; NDVI

Introduction

Land use land cover (LULC) information is essential for managing natural resources and monitoring of environmental changes. Exchanges of energy take place between the biophysical properties of the Earth (ex: vegetation) with the atmosphere. These exchanges are influenced by properties of the land, such as the overlying vegetation, the underlying soils and land management practices. Changes in these systems show adverse effect on environment by surface energy imbalance and through biogeochemical interactions that affect the carbon cycle [1]. Thus LULC changes altering the local climate are the drivers for global climate change. Increasing concentrations of greenhouse gases due to the natural and anthropogenic factors alters temperature trends [2,3]. Landscape dynamics involving LULC changes have contributed to the increase in land surface temperature (LST). The different land use types indicate the variability with different land surface temperatures (LST) [4,5]. The increasing evidence provides a base that non radiative forces such as LULC change also be major factors contributing to climate change. The climate is altered due to changes in Land use and land cover. There has been an increase in surface temperature due to alterations and conversions of vegetated surfaces to impervious surfaces [6]. These changes affect the absorption of solar radiation, surface temperature, evaporation rates, storage of heat, wind turbulence and can drastically alter the conditions of the near-surface atmosphere. The clouds, land use, land surface temperature, exchanges of energy and moisture are referred to be the key indicators considered to explain the global climate change, which vary rapidly in time and space. These parameters will drive in precise measures of radiation budget, heat balance for climate models [7]. Deforestation has been the major driver in tropics [8] and subtropics [9]. The alteration of landscapes, primarily the conversion of forests to agriculture or pasture, changes the partitioning of solar insulation into its sensible and latent turbulent heat forms. The intensified LULC changes induces prolonged drought, which can trigger large-scale landscape changes through vegetation mortality from water stress [10] and land surface conditions for decades [11,12]. The mortality of over story trees will rapidly alter ecosystem type and associated ecosystem properties at a regional-scale.

Thus, to mitigate the impacts of changes in climate, it is essential to monitor LULC changes at appropriate scales.

The investigation of environmental energy flows by thermal infrared measures of surface temperatures has been in practice since 1960's [13]. A higher level of latent heat exchange was found with more vegetated areas, while sensible heat exchange was more favored by sparsely vegetated areas. This evidence on latent heat exchange encouraged many researchers to focus on deriving LST and LULC relationship [14]. Thermal infrared (TIR) remote sensing techniques for analyzing land surface temperature (LST) patterns and its relationship with surface characteristics, assessing urban heat island (UHI), and relating LSTs with surface energy fluxes to characterize landscape properties, patterns, and processes have been well applied in urban climate and environmental studies [4-17]. However, there is limited research in complicated landscapes due to surface heterogeneity and characteristic of forests, owing to difficulties associated with sampling and quantifications. Also, there are gaps in the quantitative measures of the surface temperature heterogeneity at scales which can be recognized on the ground. The LST measures with multi temporal data at micro scale is also not addressed. The availability of remote sensing data acquired through space borne satellites (RS) and Geographic Information System (GIS) aid in the analysis of spatio-temporal dynamics of the Earth's features which help in managing natural resources and assessment of environmental changes [18]. Remote sensing through thermal scanning of entire surface types (plants and soils), simultaneously, express their temperature responses comparable to the atmospheric and radiant inputs [19,20]. An Earth surface feature emits thermal radiation at different wavelengths depending on their emissivity (ε). Emissivity is defined as the ratio of the spectral radiant emittance of a grey body to that emitted by a blackbody at the same temperature [21]. Accurate land surface emissivity values aid in reliable inferences among different land covers for retrieving LST from thermal infrared (TIR) data [6,22,23]. Land surface temperature and emissivity

***Corresponding author:** Ramachandra TV, Energy and Wetlands Research Group, CES TE15, Centre for Ecological Sciences, Indian Institute of Science, Bangalore- 560019, India, Tel: 91-80-22933099/22933503 (107); Fax: 91-80-23601428; E-mail: cestvr@ces.iisc.ernet.in

Received: August 16, 2013 **Accepted:** October 14, 2013 **Published:** October 24, 2013

are prime variables to determine the amount of thermal infrared energy radiated from the Earth's surface according to Planck's law. These variables will provide information of many different types of Earth surface processes, surface-atmosphere interactions and evapotranspiration [24].

Estimation of LST using emissivity will provide more accurate estimation with appropriate calibration of atmospheric contamination by a separation of surface emissivity and temperature from radiance at ground level and atmospheric corrections [25,26]. Earlier studies have highlighted the advantage of using TM and ETM thermal band data of Landsat sensors for deriving temperature [6,27,28]. Emissivity and LST were found to be well correlated to the measured LST [29,30]. LST derivation from the normalized difference vegetation index (NDVI) is used to derive the negative correlation between for LST downscaling purposes [31]. The NDVI cannot explain all the variation in LST and the vegetation fraction from ETM+ images is provided a stronger negative correlation than the one between LST & NDVI [29,32]. Central Western Ghats has been experiencing large scale land use changes due to many unplanned developmental activities evident from barren hilltops, conversion of perennial streams to seasonal streams, decreased flow in streams, etc. The objective of the current study is to understand LULC changes with temperature trends using multi-resolution remote sensing data. This involves,

a) Measuring the relationship between surface biophysical parameters (land use/land cover and sub-pixel thermal variations (Land Surface Temperature),

b) Determine the role land use dynamics in temperature changes through time and space.

Materials and Method

Study area

Uttara Kannada district lies between 13°55' to 15°31' N and 74°9' to 75°10' E spread over an area of 10,293 km2 in the mid-western part of Karnataka state, India (Figure 1). It is a region of gentle undulating hills, rising steeply from a narrow coastal strip bordering the Arabian Sea to a plateau at an altitude of 500 m with occasional hills rising above 600–860 m [33]. The district has 11 taluks covering three different zones i.e. coastal lands (Karwar, Ankola, Kumta, Honnavar and Bhatkal taluks), Sahyadrian interior (Supa, Yellapur, Sirsi and Siddapur taluks) and the eastern margin plains (Haliyal, Yellapur and Mundgod taluks). Uttara Kannada District has unique distinction of having different agro climatic zones and soil types. Coastal alluvial, Laterite are major soil types. According to 2011 census the ppopulation of district is 14, 36, 847 and population density is 140 persons per sq. km. From early 80's the region is started experiencing changes in land use due to the developmental activities. This conversion has occurred largely at the expense of forests and grassland [34]. Major Industrial Infrastructure of this region constitutes 8 Industrial Estates and 1 Industrial Area.

Method

Figure 2 outlines the procedure adopted in the current study. Data used in the study includes Landsat Thematic Mapper (TM) (March months of 1989, 1999), Landsat Enhanced Thematic Mapper plus (ETM+) (March 2009), and Google Earth [35]. The Survey of India topographic maps of 1:50,000 scales are used to generate base layers. The temporal remote sensing data of Landsat satellite were downloaded from the public domain [36] and geometrically corrected for the UTM coordinate system of zone 43 using GCPs (ground control points). Data are cloud free in March, transitional month from winter to summer. There are 3 India meteorological departments in the district which aided as validation stations apart from 80 locations of NOAA [37] which are well distributed and cover whole district. Field data were collected using pre-calibrated handheld Garmin GPS. The study region has vast expanse of forests, training data is collected for different forest types and other land use categories. The land cover analysis was done to assess the extent of area under vegetation, which is done through NDVI. Temporal normalised vegetation index (NDVI) is computed to assess the status of vegetation in the district. Among many indices, NDVI is most widely accepted for land cover analysis in the region dominated by vegetation cover [38,39]. NDVI is computed by using visible Red (0.0.63–0.69 μm) and NIR (0.76–0.90 μm) bands of Landsat TM. Healthy vegetation absorbs most of

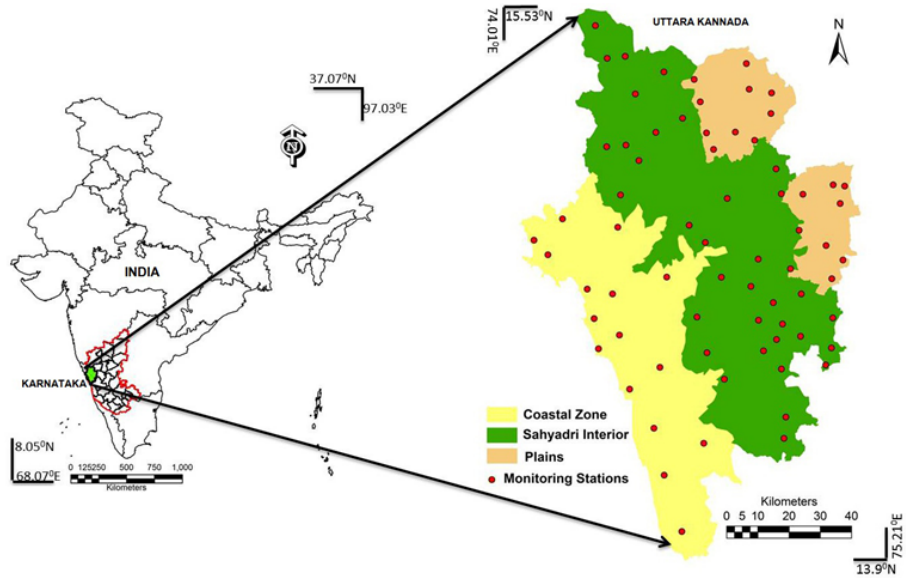

Figure 1: Study area-Uttara Kannada District.

the visible light that hits it, and reflects a large portion of the near-infrared light. Sparse vegetation reflects more visible light and less near-infrared light. NDVI ranges from minus one (-1) to plus one (+1). NDVI was calculated using Eq. (1). NDVI values range from -1 to +1 and very low values of NDVI (-0.1 and below) correspond to soil or barren areas of rock, sand, or urban built up. Zero indicates water cover. Moderate values represent low density vegetation (0.1 to 0.3), while high values indicate thick canopied vegetation (0.6 to 0.8).

$$NDVI = (NIR-R) / (NIR+R) \quad (1)$$

Land use analysis involves i) generation of False Colour Composite (FCC) of remote sensing data (bands – green, red and NIR). This helped in locating heterogeneous patches in the landscape ii) selection of training polygons (these correspond to heterogeneous patches in FCC) covering 15% of the study area and uniformly distributed over the entire study area, iii) loading these training polygons co-ordinates into pre-calibrated GPS, iv) collection of the corresponding attribute data (land use types) for these polygons from the field. GPS helped in locating respective training polygons in the field, v) supplementing this information with Google Earth [35] and Bhuvan [40], vi) 60% of the training data has been used for classification, while the balance is used for validation or accuracy assessment.

Land use analysis was carried out using supervised pattern classifier - Gaussian Maximum Likelihood Classifier (GMLC) algorithm. Remote sensing data was classified using signatures from training sites that include predominant land use types. Mean and covariance matrix are computed using estimate of maximum likelihood estimator. This technique is proved to be a superior classifier as it uses various classification decisions using probability and cost functions [41]. GRASS (Geographical Analysis Support System) a free and open source software having robust support of processing both vector, raster files has been used for this analysis. GRASS is freely accessible and downloadable [42]. The images were maintained at common resolution of 30m by downscaling. Downscaling is the enhancement of the spatial resolution of the original LST data set using ancillary information layers of superior spatial resolution [43,44]. This approach will improve the spatial details of low resolution image and obtains the image with superior resolution [26,45]. The Google earth data combined with field data is used for classification and verification of post 2000 classified image. Historical data such as French institute vegetation map [46], topographic maps were used to classify 1989, 1999 data sets. Spectral classification inaccuracies are measured by a set of reference pixels. Based on the reference pixels, confusion matrix, kappa (κ) statistics and producer's and user's accuracies were computed. The study is carried out at macro and micro scales, i.e. by considering the whole landscape as a single unit and agro-climatic zone wise analysis. The temperature estimation is done zone-wise to account agro-climatic variations.

Derivation of LST from Landsat TM

The LST values are derived in the three step process. First the image pixels of digital numbers are converted to surface radiance by including sensor specified calibration standard values. In step 2 the radiance values are again converted to equivalent range of black body temperatures. In third step the emissivity corrected temperature is derived with associated land cover type. The above specified procedure was applied separately for both sensors. The TIR band 6 of Landsat-5 TM was used to calculate the surface temperature of the area.

The digital number (DN) to radiance L_{TM} conversion

$$L_{TM} = 0.124+0.00563*DN \quad (2)$$

The radiance to equivalent blackbody temperature $T_{TMSurface}$ at the satellite using

$$TTMSurface = [K_2/(K_1-lnLTM)]-273 \quad (3)$$

The coefficients K_1 and K_2 depend on the range of blackbody temperatures, for Landsat TM $_{K1}$ = 4.127 and K_2 = 1274.7. The additional correction for spectral emissivity (ε) is required to account for the non-uniform emissivity of the land surface. Emissivity correction is carried out using surface emissivities for the specified

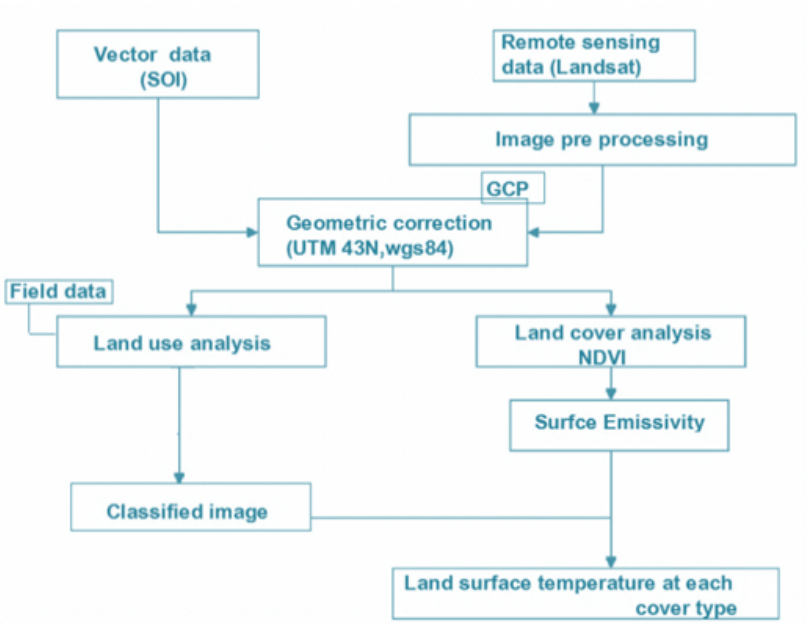

Figure 2: Method followed for LULC and LST analysis.

LC (Table 1) derived from the methodology described in [6,21]. The emissivity corrected land surface temperature (T_s) was finally computed as follows [47].

$$T_S = \frac{T_B}{1+(\lambda x T_B/\rho)\ln \epsilon} \quad (4)$$

where, λ is the wavelength of emitted radiance for which the peak response and the average of the limiting wavelengths (λ=11.5 μm) were used, ρ=h × c/σ (1.438 × 10^{-2} mK), σ=Stefan Boltzmann's constant (5.67 × 10^{-8} Wm^{-2} K^{-4}=1.38 × 10^{-23} J/K), h=Planck's constant (6.626 × 10^{-34} Jsec), c=velocity of light (2.998 × 10^{8} m/sec), and ε is spectral emissivity (Table 1).

LST from Landsat ETM+

The procedure follows same principle as done for Tm data. The TIR image Landsat ETM+ of (band 6) DN was first converted into spectral radiance L_{ETM} using equation 5, and then converted to equivalent black body temperature, $T_{ETMSurface}$, under the assumption of uniform emissivity (ε ≈ 1) using equation 6 [47,48].

$$L_{ETM} = 0.0370588*DN+3.2 \quad (5)$$

$$T_{ETMSurface} = \left[\frac{K2}{\ln\left(\frac{K1}{L_{ETM}}+1\right)}\right] \quad (6)$$

Where, $T_{ETMSurface}$ is the effective at-satellite temperature in Kelvin, LETM is spectral radiance in watts/(meters squared × ster × μm). For Landsat-7 ETM+, K_2=1282.71 K and K_1=666.09 $mWcm^{-2}sr^{-1}\mu m^{-1}$ were used. The emissivity corrected land surface temperatures T_s were finally computed by equation 4.

Results and Discussion

Temporal land cover analysis was done through NDVI reveals the transition of vegetation from 96.13 % (1989) to 89.07 % (2009). The non-vegetated areas have increased by 10.93% (2009) from 3.87% (1989). The temporal variation of land cover is shown in Table 2 and Figure 3.

Temporal land use analysis depicts land scape status and its transition from 1989 to 2009. The results show the primeval evergreen forest cover is reduced from 57.65% (1989) to 39.78% (2009) due to anthropogenic activities. Built-up area has increased from 1.13% (1989) to 2.00% (2009). The intensified agriculture activities have contributed to the decline of forests. Table 3 and Figure 4 portray the transition of landscape during 1989 to 2009.

The increase in plantation of exotic species led to the removal of primeval forest cover. Intensified cultivation and cash crop activities also aggregated the change. The accuracy assessment was included in Table 4. The field data, vegetation map and Google earth data sets are used for analysing accuracy. It shows accuracy ranges as 84.53 % (1989), 92.22 % (1999) and 89.83 % (2009).

LST computed at landscape level for both Landsat TM and ETM thermal bands as explained earlier. The minimum and maximum temperature from Landsat TM data and ETM+ data are given in

Table 1: Surface emissivity values by land cover type.

S.no	Land cover	Emissivity
1	Built-up	0.946
2	Vegetation	0.985
3	Water body	0.990
4	Agriculture	0.974
5	Others	0.950

Table 2: Land cover analysis.

Year	% vegetation	% non-vegetation
1989	96.13	3.87
1999	94.33	5.67
2009	89.07	10.93

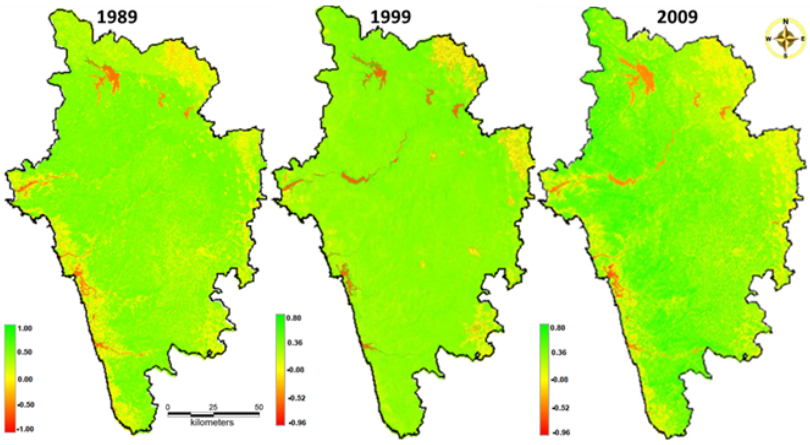

Figure 3: Temporal land cover analysis.

Table 3: Temporal land use analysis.

Year	1989		1999		2009	
Land use Category	Ha	%	Ha	%	Ha	%
Built-up	11,569	1.13	15,991	1.56	20,616	2.0
Water	19,454	1.89	26,391	2.57	28190	2.73
Crop land	175,236	17.06	170,886	16.63	185,642	18.02
Open fields	40,336	3.93	19,116	1.86	19,042	1.8
Moist deciduous forest	85,087	8.28	208,677	20.31	207924	20.18
Evergreen to semi evergreen forest	592,238	57.65	447,475	43.56	409926	39.78
Scrub/grass lands	33,843	3.29	51,439	5.01	49003	4.75
Acacia plantations	46,963	4.57	55,292	5.38	67969	6.60
Teak/Bamboo plantations	10,702	1.04	18,463	1.80	25242	2.45
Coconut_ Areca nut plantations	3001	0.29	10,839	1.06	14305	1.39
Dry deciduous forest	8831	0.86	2703	0.26	3121	0.30

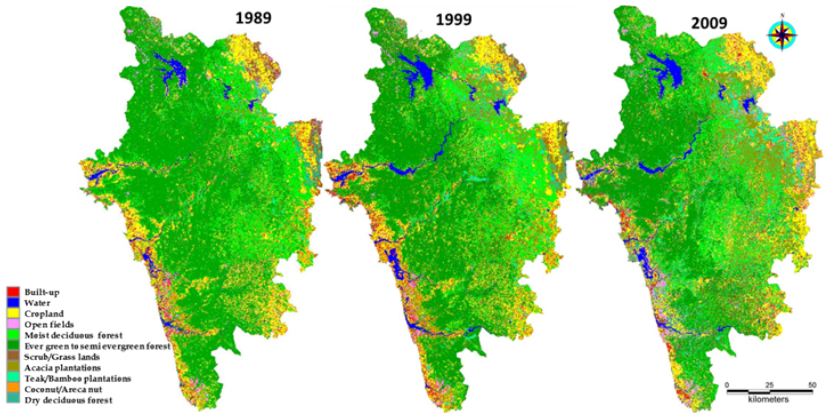

Figure 4: Supervised classification-land use analysis.

Table 5. The corresponding temperatures for all data were converted to degree Celsius. Figure 5 shows the LST map of Uttara Kannada from 1989, 1999 and 2009. Variability can be attributed to diverse landscape and higher values in recent year to the decline of forests and other human induced activities. The higher temperature can be seen especially in plains due to higher proportion of barren land and in coastal region due to intensified built-up activities. The rise in temperature can be attributed to the regions of higher deforestation and industries. The hilly regions are still maintaining moderate surface temperatures due to the presence of good vegetation cover. The region's temperature has increased from 32.7°C to 41°C; which is comparable with ground data. The same phenomenon is observed with the mean average temperature of per decade data of NASA NEO [49].

The study is done based on agro-climatic zones - 3 zones; coast, Sahyadri and plains with different levels of land cover. Figure 6 and Table 6 for the coastal region shows an increase in temperature from 31°C to 41°C due to rise in built-up areas and industrialization. The Asia's largest novel base, Kaiga nuclear project and a major industrial estate are situated in this region. The activities associated with these are the major drivers of regional temperature. It is evident from this study; the built-up and area under agriculture is increased at the loss of evergreen forest.

Figure 7 and Table 7 illustrates the role of vegetation in moderating the local temperature. Sahyadri region of the district maintain moderate rise in temperature, while plain regions with the enhanced deforestation activities show escalation in temperature. The rise in temperature can be observed due to the increase in crop lands and plantation of exotic species. Table 7 shows increase of temperature from 29°C to 37°C.

Plains in eastern and north-western parts Uttara Kannada district comprises of extensively planted teak regions and scrub type at the border of Dharwad district. It is observed that the plains are more prone to anthropogenic activities due to the proximity to urban centers. The loss of evergreen forest cover shows deforestation pattern influence on LST (Figure 8), evident from steady rise in temperature from 36 to 42°C (Table 8).

The time series analysis of air temperature is produced based on monthly average of five year time period interval from 1981-2012. The temperatures are compiled from weather data of NOAA meteorological stations measurements in and around the study region. This four-decade period functions as a baseline for the analysis. It can be inferred from the generalised curve (Figure 9) that the development of the temperature averages runs in irregular rhythm of up and downswings. A trend-like increase in air temperature overlies the cyclic fluctuations of 5 year annual temperature averages since the post 2000s. The most significant rise in air temperatures commenced in 1995-2000, post 2001 the substantial raise in air temperature is observed. The monthly average temperature from 1981-2012 also clarifies this micro level change. The situation of cyclic and trend-

Citation: Setturu B, Rajan KS, Ramachandra TV (2013) Land Surface Temperature Responses to Land Use Land Cover Dynamics. Geoinfor Geostat: An Overview 1:4.

doi:http://dx.doi.org/10.4172/2327-4581.1000112

Table 4: Accuracy assessment.

MAP2	MAP 1	1989															
	Category	Built-up	Water	Crop land	Open land	Moist deciduous	Ever green to semi	Scrub	Acacia	Teak	Coco nut	Dry deciduous	Row sum	% Commission	% Omission	PA	UA
	Built-up	110518	38	4234	617	172	89	733	372	139	786	154	117852	6.22	23.11	93.78	76.89
	Water	652	183385	3747	1607	12	291	698	20631	1250	1603	93	213969	14.29	0.58	85.71	99.42
	Crop land	23989	54	1267257	52420	97996	4407	128358	16069	25368	62569	18329	1696816	25.32	6.01	74.68	93.99
	Open land	3318	294	23260	304600	2486	1588	2353	44103	2680	1969	405	387056	21.30	21.14	78.70	78.86
	Moist deciduous	689	7	9410	3009	1008588	57697	19969	28545	52357	31852	46107	1258230	19.84	36.44	80.16	63.56
	Ever green to semi	1884	617	25031	17998	455344	5824268	17713	117922	42901	122920	6849	6633447	12.20	1.43	87.80	98.57
	Scrub	1219	23	10465	3588	7741	7271	289700	4714	4530	15208	947	345406	16.13	40.85	83.87	59.15
	Acacia	975	24	1724	1499	6824	6356	8338	381337	14926	4422	6313	432738	11.88	38.36	88.12	61.64
	Teak	169	2	151	310	3033	3163	2703	3196	91861	357	2109	107054	14.19	61.25	85.81	38.75
	Coco nut	3	0	1705	67	4520	3479	30	652	203	113931	11	124601	8.56	67.98	91.44	32.02
	Dry deciduous	324	4	1287	558	232	41	19155	1119	823	181	70171	93895	25.27	53.68	74.73	46.32
	Column Sum	143740	184448	1348271	386273	1586948	5908650	489750	618660	237038	355798	151488	11411064				
	Overall accuracy					84.53			Kappa			0.78					
MAP2	MAP 1	1999															
	Category	Built-up	Water	Crop land	Open land	Moist deciduous	Ever green to semi	Scrub	Acacia	Teak	Coco nut	Dry deciduous	Row sum	% Commission	% Omission	PA	UA
	Built-up	173333	0	0	2	0	0	14	180	974	10	73	174586	1.72	22.40	98.28	77.60
	Water	118	289130	0	2	0	0	0	449	283	258	3	290243	0.38	4.47	99.62	95.53
	Crop land	37396	0	1733799	1725	0	0	0	12436	14725	5676	3522	1809279	4.17	12.91	95.83	87.09
	Open land	4167	0	0	193784	0	0	0	9124	3609	47	862	211593	8.42	6.16	91.58	93.84
	Moist deciduous	3540	0	0	1379	2034807	42455	0	119981	70035	18330	2046	2292573	11.24	3.00	88.76	97.00
	Ever green to semi	1760	11243	176465	8075	46198	4667018	0	5471	7768	9179	776	4933953	5.41	2.16	94.59	97.84
	Scrub	666	0	0	403	0	10230	514664	20064	8208	3199	257	557691	7.72	1.84	92.28	98.16
	Acacia	784	0	0	229	0	0	0	591806	13134	1083	349	607385	2.56	25.67	97.44	74.33
	Teak	806	0	0	40	0	0	0	30096	180830	259	2200	214231	15.59	40.82	84.41	59.18
	Coco nut	655	2297	80580	870	16645	50383	9649	3422	3662	106897	233	275293	61.17	26.25	38.83	73.75
	Dry deciduous	155	0	0	0	0	0	0	3199	2354	2	24165	29875	19.11	29.93	80.89	70.07
	Column Sum	223380	302670	1990844	206509	2097650	4770086	524327	796228	305582	144940	34486	11396702				
	Overall accuracy					92.22			Kappa			0.90					

MAP2	MAP 1 Category	2009 Built-up	Water	Crop land	Open land	Moist deciduous	Ever green to semi	Scrub	Acacia	Teak	Coco nut	Dry deciduous	Row sum	% Commission	% Omission	PA	UA	
	Built-up	347785	0	0	0	0	0	0	0	0	0	0	347785	0.00	0.80	100.00	99.20	
	Water	0	311622	0	0	0	0	0	0	0	0	0	311622	0.00	0.22	100.00	99.78	
	Crop land	0	38	1574483	136	22127	0	0	12718	3273	0	0	1612775	2.37	1.85	97.63	98.15	
	Open land	0	0	0	414479	0	0	0	0	0	0	0	414479	0.00	0.93	100.00	99.07	
	Moist deciduous	0	80	5405	513	1740979	0	0	149651	43013	3	0	1939644	10.24	5.83	89.76	94.17	
	Ever green to semi	0	113	2008	1296	55625	3614057	8302	15406	0	20216	0	3717023	2.77	1.50	97.23	98.50	
	Scrub	0	48	742	58	9181	0	451649	4292	1502	2	0	467474	3.39	1.80	96.61	98.20	
	Acacia	2818	412	21495	1892	20903	54889	0	1194683	706659	0	0	2003751	40.38	13.22	59.62	86.78	
	Teak	0	0	0	0	0	0	0	0	0	0	0	0	0.00	0.00	100.00	100.00	
	Coco nut	0	0	0	0	0	0	0	0	0	523448	0	523448	0.00	3.72	100.00	96.28	
	Dry deciduous	0	0	0	0	0	0	0	0	0	0	109679	109679	0.00	0.00	100.00	100.00	
	Column Sum	350603	312313	1604133	418374	1848815	3668946	459951	1376750	754447	543669	109679	11447680					0.88
		Overall accuracy				89.83			Kappa									

Table 5: LST details.

Year	Min (°C)	Max (°C)
1989	14	32.7
1999	16	37.56
2009	17	41

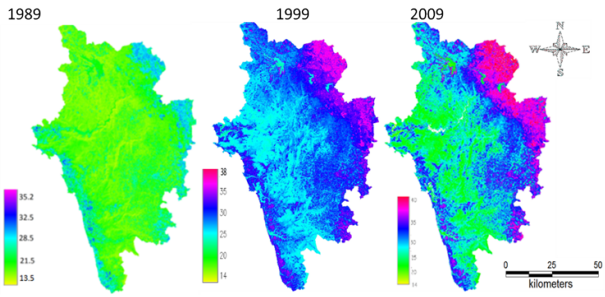

Figure 5: LST from 1989 to 2009.

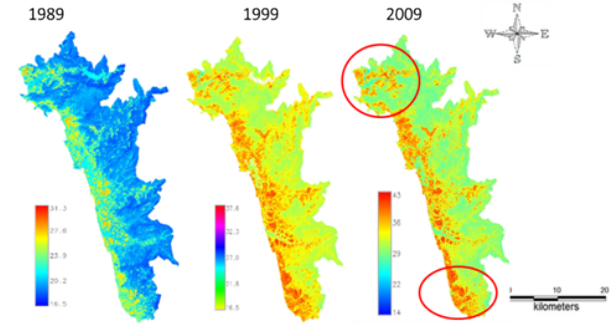

Figure 6: LST with respect to Coastal region.

Table 6: Coastal zone variations of LST.

Year	Min (°C)	Max (°C)
1989	16.49	31.34
1999	22.01	38.81
2009	22.95	42.45

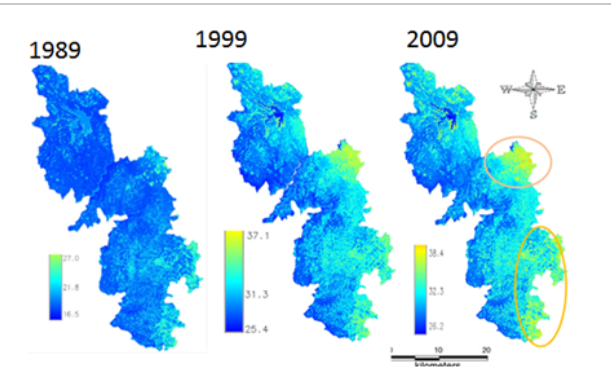

Figure 7: LST with respect to Sahyadri region.

like developments has resulted in the fact that the warming has not occurred steadily, but it is an abrupt rise due to land use changes. As outlook, the results obtained for the trend analysis have to be put in a general framework by applying the method to long-term correlations of temperature trends in order to substantiate these findings (Table 9).

Table 7: Sahyadri region LST variations.

Year	Min (°C)	Max (°C)
1989	16	29
1999	24	36
2009	26	37.2

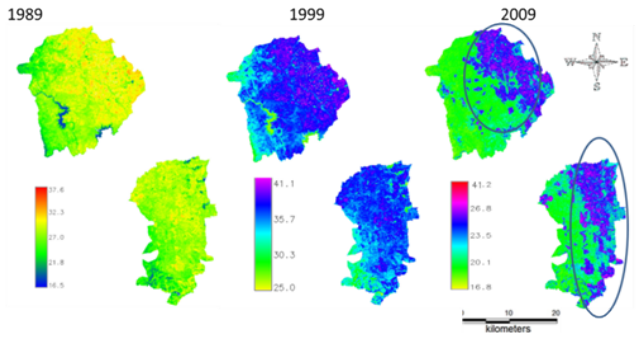

Figure 8: LST with respect to plains.

Table 8: LST of plains.

Year	Min (°C)	Max (°C)
1989	16	36
1999	25	41.2
2009	16	42

Forests in the central Western Ghats are experiencing the transition due to many developmental projects including timber, mining, power generation, etc. This has resulted in the decline of primeval evergreen forest cover from 57.65% (1989) to 39.78% (2009), which has changed LST affecting local ecology.

Conclusion

Land use changes leading to deforestation in central Western Ghats have not only altered the landscape structure but also its functioning evident from the enhanced land surface temperatures due to lack of microclimate moderation. The anthropogenic activities have altered the habitat and the impacts in the ecologically fragile region are long-term and non-reversible. Temporal land cover analysis is done through NDVI reveals the transition of vegetation from 96.13 (1989) to 89.07% (2009). Land use analysis is done using supervised classifier based on Gaussian maximum likelihood classifier reveals the decline of forests from 57.65% (1989) to 39.78% (2009). The study has related the changing land use to the changing land surface temperature at a temporal scale. Thermal signatures of different land use/land cover types in the study area helped to provide on their roles in contributing to heat phenomenon. Agro-climatic zone wise analysis illustrate that the extent vegetation in land use land cover has significant role in moderating the temperatures of a region. It is observed coastal and plain regions with lesser spatial extent of vegetation have higher temperatures than Sahyadri interior. The results indicate that there

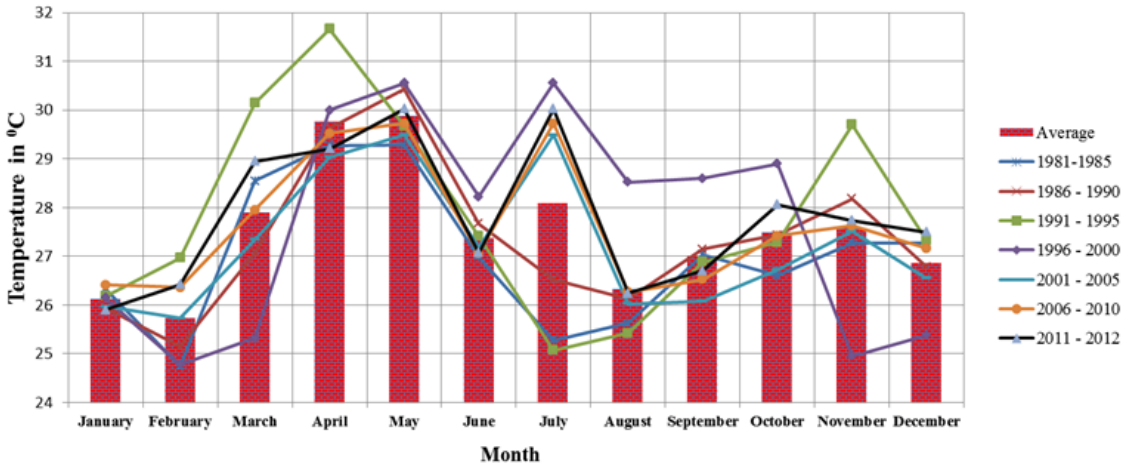

Figure 9: Ambient air temperature as recorded by weather stations from 1981 to 2012.

Table 9: Long term temperature trends.

Month	1981-1985	1986 - 1990	1991 - 1995	1996 - 2000	2001 - 2005	2006 - 2010	2011 - 2012	Average
January	26.3	25.9	26.18	26.14	25.97	26.41	25.90	26.1
February	24.7	25.1	26.97	24.78	25.73	26.36	26.42	25.7
March	28.6	27.1	30.14	25.32	27.34	27.95	28.95	27.9
April	29.3	29.6	31.67	30.00	29.04	29.52	29.20	29.8
May	29.3	30.4	29.68	30.56	29.49	29.73	30.03	29.9
June	27.0	27.7	27.42	28.23	27.18	27.06	27.07	27.4
July	25.3	26.5	25.07	30.56	29.49	29.73	30.03	28.1
August	25.6	26.1	25.42	28.52	26.03	26.27	26.24	26.3
September	27.0	27.1	26.88	28.60	26.08	26.52	26.71	27.0
October	26.6	27.4	27.29	28.90	26.73	27.42	28.06	27.5
November	27.3	28.2	29.70	24.95	27.51	27.63	27.74	27.6
December	27.3	26.8	27.34	25.38	26.55	27.17	27.50	26.9

is an increase of surface temperature from 32.74°C to 41°C. The three decadal trends in ambient air temperature also clarifies raise in temperature in recent time periods. If these changes are not addressed then there will be future drought to be occurring under warmer temperature conditions as climate change progresses, which triggers potential extent of drought-induced vegetation die-off. The results presented here suggest appropriate land use planning to mitigate the increase in temperatures by carefully crafting policies for managing anthropogenic forcing of the climate system.

Acknowledgment

We are grateful to the Ministry of Environment & Forests, the Ministry of Science and Technology (DST), Government of India, Karnataka Biodiversity Board, Western Ghats Task Force, Government of Karnataka and Indian Institute of Science for the financial and infrastructure support. We also thank Vinay S (EWRG, CES) for his help in analysing long term ground based temperature data.

References

1. Pielke RA, Marland G, Betts RA, Chase TN, Eastman JL, et al. (2002) The influence of land-use change and landscape dynamics on the climate system: relevance to climate-change policy beyond the radiative effect of green-house gases. Philos T Roy Soc A 360: 1705–1719.
2. Houghton JT, Ding Y, Griggs DJ, Noguer M, Van Der Linden PJ, et al. (2001) Intergovernmental Panel on Climate Change (IPCC). Climate Change 2001: The Scientific Basis. Cambridge University Press, Cambridge, New York, USA.
3. Trenberth KE, Jones PD, Ambenje P, Bojariu R, Easterling D, et al. (2007) Observations: surface and atmospheric climate change. Climate Change 2007: The Physical Science Basis. Cambridge University Press: Cambridge, New York, USA.
4. Weng Q, Liu H, Lu D (2007) Assessing the Effect of Land Use and Land Cover Patterns on Thermal Conditions Using Landscape Metrics in City of Indianapolis, United State. Urban Ecosyst 10: 203-219.
5. Wichansky PS, Steyaert LT, Walko RL, Weaver CP (2008) Evaluating the effects of historical land cover change on summertime weather and climate in New Jersey: part I: land cover and surface energy budget changes. J Geophys Res 113: D10107.
6. Ramachandra TV, Uttam Kumar (2010) Greater Bangalore: Emerging Urban Heat Island. GIS Development 14: 86-104.
7. Oluseyi IO, Danlami MS, Olusegun AJ (2011) Managing Land Use Transformation and Land Surface Temperature Change in Anyigba Town, Kogi State, Nigeria. Journal of Geography and Geology 3: 77-85.
8. Werth D, Avissar R (2002) The local and global effects of Amazon deforestation. J Geophys Res 107: 8087.
9. Pitman AJ, Narisma GT, Pielke RA, Holbrook NJ (2004) Impact of land cover change on the climate of southwest Western Australia. J Geophys Res 109: D18109.
10. Fensham RJ, Holman JE (1999) Temporal and spatial patterns in drought-related tree dieback in Australian savanna. J Appl Ecol 36: 1035-1050.
11. Breshears DD, Cobb NS, Rich PM, Price KP, Allen CD, et al. (2005) Regional vegetation die-off in response to global-change-type drought. National Academy of Sciences of the United States of America 102: 15144-15148.
12. Kulakowski D, Bebi P, Rixen C (2011) The interacting effects of land use change, climate change and suppression of natural disturbances on landscape forest structure in the Swiss Alps, Oikos 120: 216-225.
13. Gates DM (1962) Energy Exchange in the Biosphere, Harper and Row, New York, 151.
14. Weng Q, Lu D, Schubring J (2004) Estimation of land surface temperature–vegetation abundance relationship for urban heat island studies. Remote Sens Environ 89: 467-483.
15. Kalnay E, Cai M (2003) Impact of urbanization and land-use change on climate. Nature 423: 528-31.
16. Hung T, Uchihama D, Ochi S, YasuokaY (2006) Assessment with satellite data of the urban heat island effects in Asian mega cities. International Journal of Applied Earth Observation and Geoinformation 8: 34-48.
17. McCarthy MP, Best MJ, Betts RA (2010) Climate change in cities due to global warming and urban effects. Geophys Res Lett 37: L09705.
18. Bharath S, Bharath HA, Rajan KS, Ramachandra TV (2012) Cost effective mapping, monitoring and visualisation of spatial patterns of urbanisation using FOSS. FOSS 4G, 1st conference on open source geo-spatial technologies, Hyderabad, India.
19. Holbo HR, Luvall JC (1986) Modeling Surface Temperature Distributions in Forest Landscapes. Remote Sens of Environ 27: 11-24.
20. Moskal M, Zheng G (2012) Retrieving forest inventory variables with terrestrial laser scanning (TLS) in urban heterogeneous forest. Remote Sens 4: 1-20.
21. Stathopoplou M, Cartalis C, Petrakis M (2006) Integrating CORINE land cover data and landsat TM for surface emissivity definitions: an application for the urban area of Athens, Greece. Int J Remote Sens 28: 3291-3304.
22. Becker F, Li ZL (1995) Surface temperature and emissivity at various scales: definition, measurement and related problems. Remote Sensing Reviews 12: 225-253.
23. Dash P, Gottsche FM, Olesen FS, Fischer H (2005) Separating surface emissivity and temperature using two-channel spectral indices and emissivity composites comparison with a vegetation fraction method. Remote Sens of Environ 96: 1-17.
24. Anderson MC, Kustas WP, Norman JM, Hain CR, Mecikalski JR, et al. (2011) Mapping daily evapotranspiration at field to continental scales using geostationary and polar orbiting satellite imagery. Hydrol Earth Syst Sc 15: 223-229.
25. Li ZL, Wu H, Wang N, Qiu S, Sobrino JA, et al. (2013) Land surface emissivity retrieval from satellite data. Int J Remote Sens 9: 3084-3127.
26. Zaksek K, Ostir K (2012) Downscaling land surface temperature for urban heat island diurnal cycle analysis. Remote Sens Environ 117: 114-124.
27. Qin Z, Karnieli A, Berliner PA (2001) A mono-window algorithm for retrieving land surface temperature from Landsat TM data and its application to the Israel–Egypt border region. Int J Remote Sens 22: 3719-3746.
28. Li YY, Zhang H, Kainz W (2012) Monitoring patterns of urban heat islands of the fast-growing Shanghai metropolis, China using time-series of Landsat TM/ETM+ data. International Journal of Applied Earth Observation and Geoinfomation 19: 127-138.
29. Inadar AK, French A, Hook S, Vaughan G, Luckett W (2008) Land surface temperature retrieval at high spatial and temporal resolutions over the southwestern United States. J Geophys Res 113: 107.
30. Merlin O, Duchemin B, Hagolle O, Jacob F, Coudert B, et al. (2010) Disaggregation of MODIS surface temperature over an agricultural area using a time series of Formosat-2 images. Remote Sens Environ 114: 2500-2512.
31. Ramachandra TV, Shruthi BV (2007) Spatial mapping of renewable energy potential. Renewable and Sustainable Energy Reviews 11: 1460-1480.
32. Keramitsoglou I (2012) Advanced earth observation methodologies for the study of the thermal environment of cities. 2nd International Workshop EORSA 11-15.
33. Yang G, Pu R, Huang W, Wang J, Zhao C (2010) A novel method to estimate sub-pixel temperature by fusing solar-reflective and thermal-infrared remote sensing data with an artificial neural network. IEEE Trans Geosci Remote Sens 48: 2170-2178.
34. Ramachandra TV, Kumar U, Aithal, Diwakar PG, Joshi NV (2010) Landslide Susceptible Locations in Western Ghats: Prediction through Open Modeller. 26th Annual In-House Symposium on Space Science and Technology, ISRO-IISc Space Technology Cell, Indian Institute of Science, Bangalore, 65-74.
35. Google Earth.
36. Landsat.org.
37. NOAA.
38. Weismiller RA, Kristof SJ, Scholtz DK (1977) Change detection in coastal zone environments. Photogram Eng Remote Sensing 43: 1533-1539.

39. Nelson RF (1983) Detecting forest canopy change due to insect activity using Landsat MSS. Photogram Eng Remote Sensing 49: 1303-1314.

40. Bhuvan.

41. GRASS.

42. Ramachandra TV, Setturu B, Bharath HA (2012) Peri-Urban to Urban Landscape Patterns Elucidation through Spatial Metrics. International Journal of Engineering Research and Development 2: 58-81.

43. Bechtel B, Zaksek K, Hoshyaripour G (2012) Downscaling land surface temperature in an urban area: A case study for Hamburg, Germany. Remote Sens 4: 3184-3200.

44. Stathopoulou M, Cartalis C (2009) Downscaling AVHRR land surface temperatures for improved surface urban heat island intensity estimation. Remote Sens Environ 113: 2592-2605.

45. Gao F, William PK, Martha C, Anderson A (2012) Data Mining Approach for Sharpening Thermal Satellite Imagery over Land. Remote Sens 4: 3287-3319.

46. Pascal JP (1986) Explanatory booklet on the forest map of South India. French Institute, Pondicherry 3: 19-30.

47. Artis DA, Carnahan WH (1982) Survey of emissivity variability in thermography of urban areas. Remote Sens Environ 12: 13-329.

48. Landsat Project Science Office and the data (2002).

49. NASA NEO.

Author Affiliation

Top

[1]*Energy and Wetlands Research Group, Centre for Ecological Sciences (CES), Bangalore, India*

[2]*Lab of Spatial Informatics, IIIT-H, Hyderabad, India*

[3]*Centre for Infrastructure, Sustainable Transportation and Urban Planning (CiSTUP), Indian Institute of Science, Bangalore, Karnataka, India*